Polymer 51 (2010) 2125–2132

Contents lists available at ScienceDirect

Polymer

journal homepage: www.elsevier.com/locate/polymer

# The synthesis and characterization of functional poly(citraconic anhydride-*co*-styrene-*co*-vinylphosphonic acid)s

Serap Kavlak [a], Ali Güner [a,*], Zakir M.O. Rzaev [b]

[a] Hacettepe University, Faculty of Science, Department of Chemistry, 06800 Beytepe, Ankara, Turkey
[b] Hacettepe University, Faculty of Engineering, Department of Chemical Engineering, 06800 Beytepe, Ankara, Turkey

ARTICLE INFO

*Article history:*
Received 4 November 2009
Received in revised form
4 March 2010
Accepted 7 March 2010
Available online 15 March 2010

*Keywords:*
Radical polymerization
Structure-property relation
Vinylphosphonic acid

ABSTRACT

New functional terpolymers of citraconic anhydride (CA), styrene (S) and vinylphosphonic acid (VPA) were synthesized at different compositions by complex-radical ternary polymerization. Studied ternary acceptor-donor-acceptor system was described as a binary copolymerization of two monomer complexes of CA…S (1) and VPA…S (2). The monomer reactivity ratios of these complexes were determined by $^1$H NMR analysis for monomer mixtures before and after reactions by modified Jaacks equations: $r_1 = r_1(K_{c1}/K_{c2}) = 1.99$, $r_{II} = r_2(K_{c2}/K_{c1}) = 0.16$; $r_1 = 18.59$, $r_2 = 0.018$ (taking into account $K_c$ for the corresponding monomer complexes). Copolymerization constants verify the fact that complexed monomer pairs have a tendency towards random copolymerization. Monomer unit compositions and characterizations of a series of poly(CA-*co*-S-*co*-VPA)s were investigated by FTIR, Raman, $^1$H NMR, $^{13}$C NMR, DEPT-135, $^{31}$P NMR, GPC and thermal properties were investigated by TGA and DSC methods. Molecular weight and thermal stability increased with increasing VPA content in terpolymer. Dynamic mechanical properties were investigated by DMA and all terpolymers show typical viscoelastic behavior of an amorphous polymer. Solution properties were also studied by viscometry and titration.

© 2010 Elsevier Ltd. All rights reserved.

## 1. Introduction

Recently polymers containing pendant phosphonic acid groups have attracted a special attention. Previously, studies on poly(vinylphosphonic acid-*co*-acrylamide) hydrogels [1], poly(styrene-*co*-vinylphosphonic acid) ionomers [2], proton exchange membranes of blends of PPO with poly(styrene-*b*-vinylbenzylphosphonic acid) copolymers [3], copolymers of vinylphosphonic acid with 1-vinyl-2-pyrrolidone [4], poly(vinylphosphonic acid) [5], a proton-conducting solid electrolyte membrane based on poly(vinylphosphonic acid) and 3-glycidoxypropyltrimethoxysilane [6], styrene, spiro-orthoester with an acrylate group and diethyl (methacryloyloxymethyl) phosphonate terpolymer [7] have been reported in literature.

Complex-radical copolymerization of donor-acceptor multicomponent systems is an effective method for the synthesis of functional macromolecules with a given composition and special properties. Binary and ternary systems containing acceptor and donor monomers can be synthesized by complex-radical copolymerization method [8]. Citraconic anhydride-styrene and citraconic anhydride-maleic anhydride-styrene terpolymer [9,10], complex-radical copolymerization of *p*-vinylphenyl boronic acid with maleic anhydride and citraconic anhydrides [11], copolymers of *tert*-butyl vinyl ether with maleic and citraconic anhydrides [12] have been synthesized previously.

Ternary monomer systems containing electron-donor (D) and electron-acceptor (A) monomers can be classified by the $D_1-D_2-D_3$ (1), $A_1-A_2-A_3$ (2), $D_1-A-D_2$ (3) and $A_1-D-A_2$ (4). Donor-acceptor monomer pairs can be present in forms of $D_1$…A and $D_2$…A complexes or $A_1$…D and $A_2$…D complexes for (3) and (4) systems in initiation, propagation, termination and chain transfer reactions. Functional groups of these monomers can be formed in H-complexes of monomer mixtures. These systems can be described as a binary copolymerization of two complexed monomers [8,13–19].

In this study, $A_1-D-A_2$ monomer system were investigated and novel functional terpolymers of citraconic anhydride (CA) and styrene (S) with vinylphosphonic acid (VPA) were synthesized with certain compositions by complex-radical terpolymerization. In order to investigate polymerization reactions, complex formation constant and the complexed monomer reactivity ratios were determined by $^1$H NMR analysis. Monomer unit compositions, characterization and structure-property relationships of poly(citraconic anhydride-*co*-styrene-*co*-vinylphosphonic acid)s {poly(CA-*co*-S-*co*-VPA)s} were investigated with GPC, FTIR, Raman, $^1$H NMR, $^{13}$C NMR, DEPT-135, $^{31}$P NMR, TGA, DSC, DMA, viscometry and titration methods.

* Corresponding author. Fax: +90 312 2992163.
*E-mail address:* agun@hacettepe.edu.tr (A. Güner).

0032-3861/$ – see front matter © 2010 Elsevier Ltd. All rights reserved.
doi:10.1016/j.polymer.2010.03.016

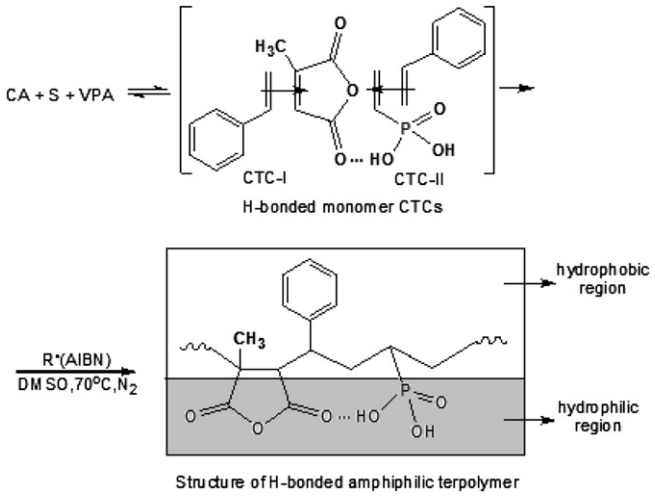


**Scheme 1.** Terpolymerization of CA, S and VPA via monomer CTCs.

The pathway of the synthesis of terpolymers can be presented in Scheme 1.

## 2. Experimental section

### 2.1. Materials

VPA (Fluka) monomer was used without further purification. mp. 41–45 °C, $d_4^{20}$ 1.409, $n_D^{20}$ 1.473. FTIR spectrum (KBr pellet, $cm^{-1}$): above 3000 (C–H stretching mode bands due to the vinyl- group), 3200–2900 (b, O–H bending bands of intramolecular H-bonds), 2700–2600 (PO–H stretching), 2360–2200 (b, combination of POH bending and the asymmetric stretching of O–P–O). 1614 (C=C stretching), 1409 (s, $CH_2$ scissoring), 1279 (w, CH in-plane bending), 1126 (b, P=O stretching), 1025 (an asymmetric O–P–O stretching), 944 (O–P–O symmetric stretching frequency). Raman spectrum ($cm^{-1}$): above 3090 (w, O–H stretching bands), 2876 (b,s, C–H stretching vibration), 2374 (s,b, P–H stretching), 1224 (P=O stretching), 936 ν(O–P–O). $^1$H NMR spectrum (DMSO-$d_6$, at 25 °C, ppm): $\delta$ = 8.50 (OH–, 2H singlet), 6.18–6.05 (C–H = , 1H quartet), 5.99–5.78 ($H_2C$=, 2H quartet).

S (Aldrich) monomer was purified before use by distillation under vacuum. CA (Fluka) monomer was used without further purification.

2,2′-Azobisisobutyronitrile (AIBN) (Fluka) was recrystallized from methanol and was dried under vacuum. The solvents were analytical grade and used as received.

### 2.2. Complex formation in monomer system

Charge transfer complex (CTC) formation constant ($K_c$) for the for the S-CA complex was determined by the $^1$H NMR spectroscopy in DMSO-$d_6$, at 25 °C; $^1$H NMR spectra of pure monomer and mixtures (CA:$S$ = 1:5, 1:10, 1:20, 1:30 mol %) ([S]>>[CA]) = 0.1 mol $L^{-1}$, [S] = 0.5, 1.0, 2.0 and 3.0 mol $L^{-1}$ with an excess of electron-donor monomer (S) show an appreciable displacement in chemical shifts of electron-acceptor monomer.

### 2.3. Synthesis of poly(CA-co-S-co-VPA)s

The radical terpolymerizations of CA with S and VPA at certain monomer feed ratios (40:50:10, 25:50:25, 10:50:40 mol %) were performed in 70 wt. % solutions of monomers in DMSO, using AIBN (1.0%, based on the total weight of monomers) as initiator. For polymerizations standard conditions were used as follows: Narrow neck tubes were charged with appropriate quantities of monomers, DMSO and AIBN. To reduce the influence of oxygen, tubes were flushed with nitrogen gas. The solution was heated to 70 °C and stirred at this temperature for 24 h, under nitrogen atmosphere. At the end of the reaction polymer mixtures were cooled to room temperature and polymers were separated by precipitation with methanol, and then washed with several portions of diethyl ether and finally reprecipitated from acetone solution. Resultant polymers were dried under vacuum.

The poly(CA-*co*-S-*co*-VPA)s are systematically named according to the monomer feed ratio of terpolymers such as terpolymer-1 (40:50:10 mol %), terpolymer-2 (25:50:25 mol %) and terpolymer-3 (10:50:40 mol %).

### 2.4. Determination of the complexed monomer reactivity ratios

To determine the reactivity ratios terpolymerizations of CA with S and VPA at certain monomer feed ratios CA…S: VPA…$S$ = 80:20 mol % (CA:S:VPA = 40:50:10 mol %) and CA…S:VPA…$S$ = 20:80 mol % (CA:S:VPA = 10:50:40 mol %) were achieved up to a low conversion at the same conditions. Terpolymerization reactions of the prepared monomers were performed inside NMR equipment using deuterated DMSO as a solvent before and after reaction at 70 °C for 5.5 h. To reduce the influence of oxygen, tubes were flushed with nitrogen gas before polymerization.

### 2.5. Measurements

The FTIR spectra of monomers were recorded with a Perkin Elmer FTIR spectrometer in the 4000–400 $cm^{-1}$ range by signal averaging a total of 8 scans, with a resolution of 1 $cm^{-1}$. Samples were prepared by mixing the polymers with KBr (1:9 wt.-%) powder. Disks were prepared by pressing the mixture using a press at room temperature. The Raman spectra of monomers were obtained with a Jobin-Yvon LabRam HR800 Raman spectrometer equipped with a charge coupled device (CCD) detector using the 632.8 nm line of a He–Ne nm laser. The powdered samples were pressed onto a microscope slide. The laser was focused onto sample surface by means of a microscope (Olympus BX41). Samples were recorded with a 3 accumulation, 400s (objective × 100, grating 600). For investigating the complex formation constants and structural identifications $^1$H, $^{13}$C NMR spectra were collected for monomers and monomer pairs using a Bruker 400 MHz NMR spectrometer. For the $^1$H, $^{13}$C analysis TMS was used as the internal standard whereas for $^{31}$P NMR analysis $H_3PO_4$ was used.

Molecular weights of terpolymers were determined by PL-GPC 220 GPC equipment in THF at 30 °C. The column oven can comfortably hold two 30 cm GPC columns, refractive index (RI) detector and injection valve, as well as a viscometer and two-angle (15° and 90°) light scattering detector. Narrow polydispersity index exists where anionically synthesized polystyrenes are used for universal calibration.

Thermogravimetric and Differential Thermal Analysis of polymers were performed with a Shimadzu TA-60 WS Thermal Analyzer. Thermal degradation of the polymers was investigated under nitrogen atmosphere with a heating rate of 10 °C/min from 30 to 500 °C. Thermal transitions of the polymers were investigated by Shimadzu DSC-60 Instruments under nitrogen atmosphere with a heating rate of 10 °C/min, from 30 to 300 °C. Glass transition temperatures were determined from the second heating run of the mid points.

Dynamic mechanic behaviors of terpolymers were performed by TA Q800 Dynamic Mechanic Analyzer. Mixtures of polymer and

$Al_2O_3$ (50:50 wt. %) were prepared and these powdered mixtures were loaded into the DMA using a novel powder-holder, which consisted of upper and lower trays of stainless steel. The holder was clamped directly into the DMA dual cantilever rig and tightened to 6 PSI torque using the torque tool. The temperature dependence of polymers was measured at a constant frequency ($\omega = 1$ Hz) using a standard temperature sweep (3 °C/min) from −50 to 250 °C. These temperature ranges were achieved by initially cooling the DMA using a liquid nitrogen accessory.

Viscosity behaviors of terpolymers were performed by Ubbelohde type capillary viscometer at 25 ± 0.1 °C, in DMF. Acid numbers of terpolymers were determined by the known titrimetric method [20].

## 3. Results and discussion

### 3.1. Charge-transfer complex formation

$^1$H NMR spectra of pure monomer and its mixtures (CA:S) with an excess of electron-donating monomer (S >> CA) show an appreciable displacement of chemical shifts of maleic anhydride protons at 25 °C ($\delta_{CH} = 7.0884$ ppm) to the strong field ($\delta_{CH} = 7.0884–6.9906$ ppm) with a chemical shifts values of 0.0160, 0.0277, 0.0599, 0.0978 ppm for increasing S concentration. The changes for chemical shifts with a significant excess of S allow the determination of the equilibrium constant ($K_c$) of complexation. The value of $K_{c1} = 0.049 \pm 0.1$ L mol$^{-1}$ for CA:S at 25 °C was found from the graphical relationship $\Delta_{obs}^{-1}$ (ppm$^{-1}$) → 1/[D]$_0$ according to the Hanna-Ashbaugh [21] relation. From the donor-acceptor properties of the studied monomers, it may be predicted that the formation of the following equimolar (1:1) CTCs between in the CA:S system as may occur shown in below:

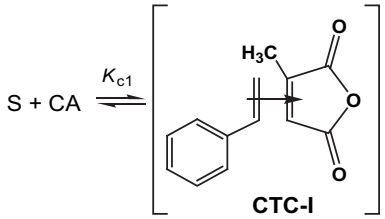


Complex formation constant of the VPA-S monomer pair was found previously from the $^1$H NMR analysis as $K_{c2} = 0.458 \pm 0.1$ L mol$^{-1}$ in DMSO-$d_6$, at 25 °C [22].

### 3.2. Complexed monomer reactivity ratios

Terpolymerizations of donor and acceptor monomer systems can be described as a binary copolymerization system of two different monomer charge transfer complexes where terpolymerizations occur via both free and complexed monomers. Terpolymerizations were carried out up to low conversions as low as (≤10%) in order to determine the monomer reactivity ratios in the steady-state kinetics by using known modified Jaacks equations (Eqs. (1)–(2)) [23]. The modified Jaacks method was preferentially applied since it involves the use of a large excess of one monomer pair relative to the other in order to consider only one growing radical:

$$\log([Am_1]_t/[Am_2]_0) = r_I \cdot \log([Am_2]_t/[Am_2]_0) \text{ for } [CA\ldots S] < < [VPA\ldots S] \quad (1)$$

$$\log([Am_2]_t/[Am_2]_0) = r_{II} \cdot \log([Am_1]_t/[Am_1]_0) \text{ for } [VPA\ldots S] < < [CA\ldots S] \quad (2)$$

where $[Am_i]_0$ and $[Am_i]_t$ are the integral areas of −C=CH- protons of CA, $-CH_2$ = CH- protons of S and $-CH_2$ = CH- protons of VPA monomers before and after polymerization at low conversion conditions used for a given time $t$, respectively, clearly observed in $^1$H NMR spectra (Fig. 1) and Table 1. Analysis of constants of copolymerizations, with regard to the constants of CTC formation, provides that the VPA…S complex is more active in the radical copolymerization as compared to CA…S complex in the CA-S-VPA system: $r_I = r_1(K_{c1}/K_{c2}) = 1.99$, $r_{II} = r_2(K_{c2}/K_{c1}) = 0.16$; $r_1 = 18.59$, $r_2 = 0.018$ (taking into account $K_{c1}$ and $K_{c2}$ constants). The effect of the values of copolymerization constants on the reactivity of the monomers obtained by taking into considerating the variation of $K_c$, verify the fact that complexed monomer pairs have a tendency towards random copolymerization. It can be proposed that, copolymerization of complexation proceeds with random mechanism of the S…CA and S…VPA units.

### 3.3. Spectroscopic characterization of poly(CA-co-S-co-VPA)s

Compositions of terpolymers were determined by FTIR spectroscopy. The absorption value ratios between characteristic analytical bands of 1779–1767 cm$^{-1}$ (for CA unit), 705–698 cm$^{-1}$ (for S unit), 947–944 cm$^{-1}$ (for VPA unit) and the least changing absorption band of 548 cm$^{-1}$ as a standard band $A = \log(I_0/I)$ were used to calculate the terpolymer compositions. Molar fractions (in mol %) of monomer units ($m_1$, $m_2$ and $m_3$) in CA($M_1$)-S($M_2$)-VPA($M_3$) terpolymers using FTIR analysis data were calculated according to the Eqs. (3)–(5) [24]:

$$m_1 = \frac{\Delta A^{1767}/M_1}{\Delta A^{1767}/M_1 + \Delta A^{705}/M_2 + \Delta A^{945}/M_3} \times 100 \quad (3)$$

$$m_2 = \frac{\Delta A^{705}/M_2}{\Delta A^{1767}/M_1 + \Delta A^{705}/M_2 + \Delta A^{945}/M_3} \times 100 \quad (4)$$

$$m_3 = \frac{\Delta A^{945}/M_3}{\Delta A^{1767}/M_1 + \Delta A^{705}/M_2 + \Delta A^{945}/M_3} \times 100 \quad (5)$$

where $\Delta A = A^i/A^{548}$ (standard band); $M_1$, $M_2$, and $M_3$ are molecular weights (g mol$^{-1}$) of CA, S and VPA monomer units, respectively. Compositions of CA, S and VPA in terpolymers are summarized in Table 2. For these analyses relatively high conversions were used. Different reactivity and relatively high conversion can be the reason of relatively similar terpolymer composition reported in Table 2. In this system especially in equimolar composition CTCs can be more effective but in other compositions polymerizations occurred by the way of both free and complexed monomers. H-bonding is another important factor in this system. There are interactions due to the inter- and intramolecular H-bonding between CA and VPA units, respectively. Consequently, there are competitions in these ternary systems resulted to nearly the same compositions.

Spectroscopic techniques were used to analyze the structure and properties of terpolymers in detail. Spectral studies provide important clues about the terpolymerization, structural analysis and characterization of polymers. FTIR spectra of terpolymers are presented in Fig. 2. The strong absorption bands at 696–760 cm$^{-1}$ correspond to mono-substituted benzene ring of styrene units. The broad and strong bands between 947 and 1069 cm$^{-1}$ correspond to the symmetric and asymmetric P–O(H) bands of phosphonic acid

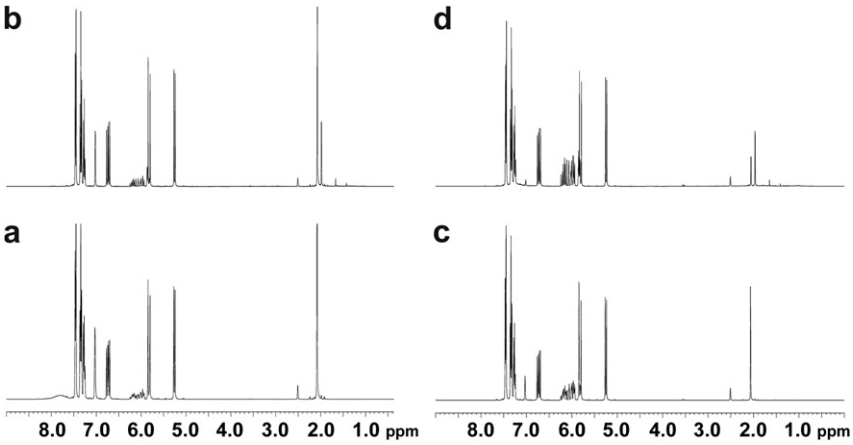


**Fig. 1.** $^{1}$H NMR spectra of monomer mixtures of CA…S:VPA…$S$ = 80: 20 mol % before (a) and after (b); CA…S:VPA…$S$ = 20: 80 mol % before (c) and after (d) reaction at 70 °C for 5.5 h in DMSO-$d_6$.

units. Another characteristic band of phosphonic acid units appears at 1183 cm$^{-1}$ and corresponds to a P=O stretching for all terpolymers. The peak at 1221–1228 cm$^{-1}$ represents the C–O stretching of maleic anhydride units. The bands at ~1600 cm$^{-1}$ belong to the aromatic rings of styrene units. C=O asymmetric and symmetric stretching bands and C=O overtones appear at 1954–1775 cm$^{-1}$. Broad O–H stretching bands of the free and H-bonded O–H appear at 2570 cm$^{-1}$ and a range of 2920–3619 cm$^{-1}$. The peaks corresponding to the POH bending and O–P–O asymmetric stretching are observed at 2320–2325 cm$^{-1}$ [25].

Raman spectra (between 900 and 1300 cm$^{-1}$) of terpolymers for different compositions are shown in Fig. 3. Bands in the range of 357–734 cm$^{-1}$ belong to the skeletal deformation. Characteristic bands of phosphonic acid, styrene and citraconic anhydride units appear at 630–1100 cm$^{-1}$ and these bands resulted from different vibration modes of $PO_2$, $PO_3$, P–C, C–C, C–O, C–O–C, $CH_2$ and P–O. Bands observed in the 929–982 cm$^{-1}$ region belong to the symmetric and asymmetric P–O stretching. Bands belonging to anhydride units appear with weak intensity. The band at 3000–2800 cm$^{-1}$ belongs to C–H stretching mode on the polymer chain. Spectrum of the terpolymer-3 has a much weaker intensity, probably, due to the nature of the powdered form.

$^{1}$H NMR spectra of terpolymers are presented in Fig. 4(A). In spectra, the aromatic protons of styrene unit appear at 7.48–6.63 and 7.46–6.34 ppm (5H, S), unreacted VPA monomer is observed at 6.14–5.81 ppm, CH proton of VPA, CH proton of S and CH proton of CA units center at 3.41 and 3.37 ppm (1H, VPA; 1H, S; 1H, CA), $CH_2$ protons of the backbone belonging to S are displayed in the range of 2.10–1.44 and 2.09–1.30 ppm (2H, S) and the peaks at 0.97 and 1.12–0.37 ppm correspond to the $CH_2$ protons of the backbone belonging to VPA and $CH_3$ protons of the CA (2H, VPA, 3H, CA) for the terpolymer-1 and terpolymer-2, respectively.

$^{13}$C NMR spectra (in DMSO-$d_6$) of the terpolymers are presented in Fig. 4(B). The peaks at 174.15 and 176.50 ppm correspond to the carbon atom of C=O group in CA units (1C, CA), another peak for the carbon atom of C=O group of CA units appears at 171.65 and 172.20 ppm (1C, CA). The peaks centered at 140.85 and 141.00 ppm can be attributed to the carbon atom of the 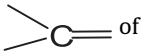 of styrene (1C, S) whereas carbon atom of the CH of VPA unit appears at 59.64 and 59.47 ppm (1C, VPA) and CH peak of CA can be observed at 48.51 and 48.32 ppm (1C, CA), carbon atom of the $CH_2$ of backbone and carbon atom of the CA overlap and can be observed at 42.97 and 43.00 ppm (1C, S and 1C, CA). Other carbon atom of the $CH_2$ group of the backbone appears at 37.50 (1C, VPA), CH of the S unit appears at ~21 ppm (1C, S) and carbon atom of the $CH_3$ group of the CA unit appears at 20.64 and 20.89 ppm, for the terpolymer-1 and terpolymer-2, respectively.

DEPT-135 spectra of terpolymer-1 and terpolymer-2 are shown in Fig. 4(C) and peak assignments are also presented in the same figure. More intense signal was obtained from DEPT-135 spectra. The peaks attributed to 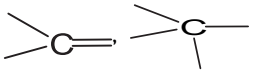 and C=O are completely absent in the spectrum. As positive signals indicate the methine carbon, negative signals indicate the methylene carbon atoms in DEPT-135 spectrum.

$^{31}$P NMR spectra of terpolymers are presented in Fig. 5. Terpolymers show resonance at 29.07 and 29.41 ppm, for the terpolymer-1 and terpolymer-2, respectively, due to the phosphonic acid groups. Broad peaks were observed due to the sequential distribution of the comonomers. The peaks in the region of 11.76 ppm are observed due to the unreacted or complex bound VPA monomers.

**Table 1**
$^{1}$H NMR analysis data of CA/S/VPA monomer mixtures before and after polymerization for the determination of the monomer reactivity ratios by the modified Jaacks equations.

| Monomer feed (mol %) | | Integral area of CA -CH = C- protons | | Integral area of S -$CH_2$ = CH- protons | | Integral area of VPA -$CH_2$ = CH- protons | |
|---|---|---|---|---|---|---|---|
| [CA…S] | [VPA…S] | $[Am_1]_0$ | $[Am_1]_t$ | $[Am_2]_0$ | $[Am_2]_t$ | $[Am_3]_0$ | $[Am_3]_t$ |
| 80 | 20 | 0.1500 | 0.0996 | 0.1988 | 0.1952 | 0.0285 | 0.0260 |
| 20 | 80 | 0.0416 | 0.0206 | 0.1988 | 0.1902 | 0.0386 | 0.0320 |

**Table 2**
FTIR analysis for the determination of composition of terpolymers.

| Monomer feed (mol-%) | | | $\Delta A^{1767}$ CA-unit | $\Delta A^{705}$ S-unit | $\Delta A^{945}$ VPA-unit | Terpolymer composition (mol-%) | | |
|---|---|---|---|---|---|---|---|---|
| CA ($M_1$) | S ($M_2$) | VPA ($M_3$) | | | | CA ($m_1$) | S ($m_2$) | VPA ($m_3$) |
| 40 | 50 | 10 | 0.941 | 0.854 | 0.868 | 34.08 | 33.29 | 32.62 |
| 25 | 50 | 25 | 0.930 | 0.900 | 0.941 | 32.35 | 33.69 | 33.96 |
| 10 | 50 | 40 | 0.876 | 0.819 | 1.057 | 30.70 | 30.89 | 38.78 |

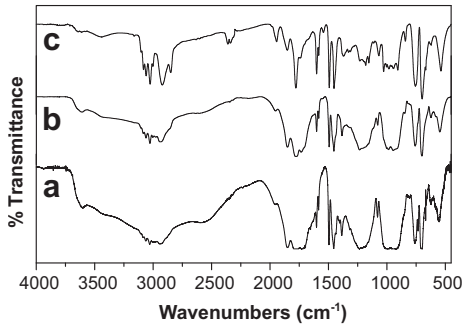


**Fig. 2.** FTIR spectra of the terpolymers, (a) terpolymer-1, (b) terpolymer-2 and (c) terpolymer-3.

### 3.4. GPC analysis

The molecular weight distribution plots are presented in Fig. 6 and the molecular weight averages and polydispersity indexes (PDIs) are summarized in Table 3. Increasing the VPA content in the feed increases the molecular weights of the terpolymer. It can be explained by the complexation tendencies of the monomers. VPA behaves as the complexing agent and increases the activity of the CA monomer.

### 3.5. Thermal analysis

TGA curves of terpolymers are shown in Fig. 7(a). Terpolymer-1 and terpolymer-2 undergo two step and terpolymer-3 undergoes one step decomposition. First steps of degradations are observed at 71–183 °C with a 12% weight loss and at 123–201 °C with a 5.5% weight loss for terpolymer-1 and terpolymer-2, respectively. Peak minima were observed at 124.1 °C and 163.5 °C from DTG curves for these terpolymers. Evolution of physically bound water from terpolymers and water released from the anhydride formation of P–OH units can explain these weight losses. Main degradations are observed at high temperatures for the series of these terpolymers. During the second degradation, large weight loss of 81.6% from 281 to 444 °C and 87.5% from 270 to 437 °C appeared. According to Fig. 7

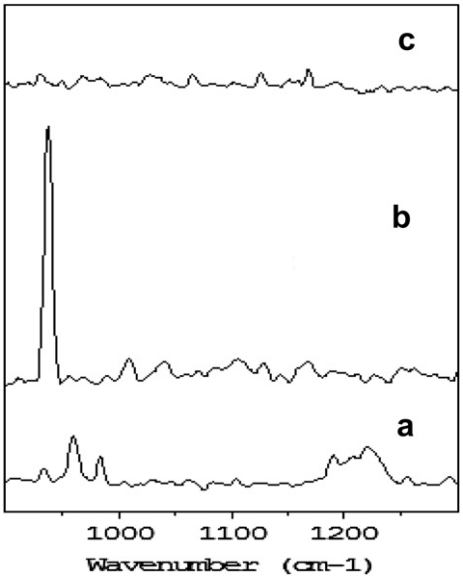


**Fig. 3.** Raman spectra of terpolymers, (a) terpolymer-1, (b) terpolymer-2 and (c) terpolymer-3, obtained between 900 and 1300 $cm^{-1}$, using the 632.8 nm line of a He-Ne laser.

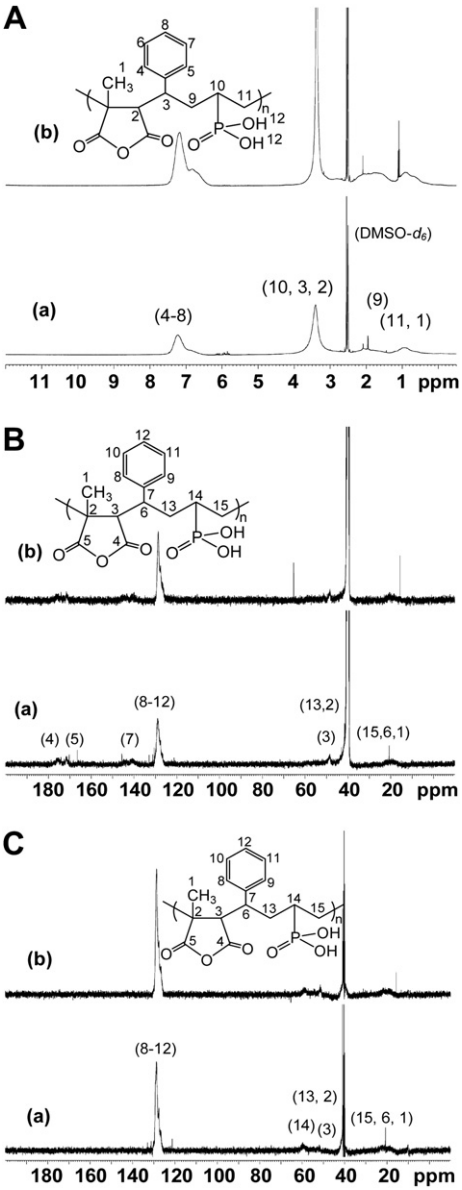


**Fig. 4.** $^{1}H$ NMR (A), $^{13}C$ NMR (B) and DEPT-135 NMR (C) spectra of terpolymers (a) terpolymer-1, (a) terpolymer-2 in DMSO-$d_6$.

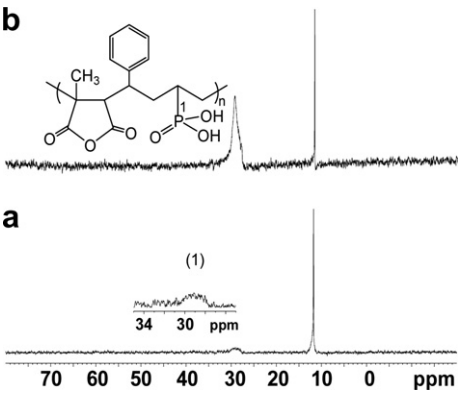


**Fig. 5.** $^{31}P$ NMR spectra of terpolymers, (a) terpolymer-1, (b) terpolymer-2 in DMSO-$d_6$.

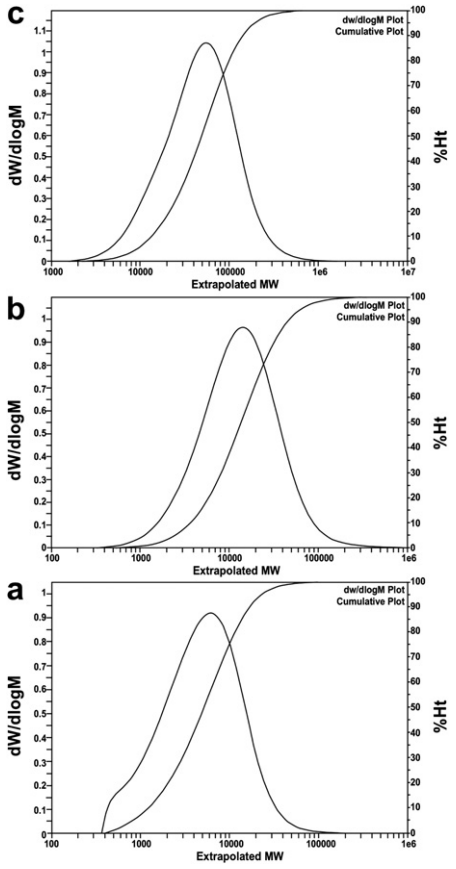


**Fig. 6.** Molecular weight plots of the terpolymers, (a) terpolymer-1, (b) terpolymer-2 and (c) terpolymer-3.

(b) first derivative curves show peaks at 374.8 °C and 387.3 °C with a minimum for the maximum degradation temperatures. A small weight loss of 2.6% is observed up to 300 °C and can be related to the loss of physically bound water from the terpolymer-3. This terpolymer degrades essentially in the temperature range from 300 °C to 465 °C with the weight loss of 96.9%. Weight losses at these high temperatures for all terpolymers may result from major condensation of anhydride formation of phosphonic acid units, aromatic ring decomposition belonging to styrene units such as formation of toluene and benzene. In addition, main chain degradations and C–P breaking are responsible for these weight losses. Weight losses of 88.8, 87.2 and 17.0% were observed for terpolymer-1, terpolymer-2 and terpolymer-3, respectively, up to 400 °C. At the end of 500 °C, it can be said that all terpolymers are decomposed completely. The higher thermal stability is observed for terpolymer-3 up to 380 °C.

DSC curves are shown in Fig. 7(c). Glass transition temperatures of terpolymer-1 and terpolymer-3 were observed at 114 and 112 °C; for terpolymer-2 glass transition temperature was not observed exactly because of the overlapping with the peak of pseudo-melting.

**Table 3**
Average molecular weights of terpolymers obtained from GPC analysis.

| Parameter | Terpolymer-1 | Terpolymer-2 | Terpolymer-3 |
|---|---|---|---|
| $\overline{M}_n$(g.mol$^{-1}$) | 2800 | 7700 | 28,800 |
| $\overline{M}_w$(g.mol$^{-1}$) | 7400 | 20,700 | 66,700 |
| $\overline{M}_z$(g.mol$^{-1}$) | 16,700 | 63,300 | 138,900 |
| PDI | 2.62 | 2.69 | 2.32 |

PDI: Polydispersity index.

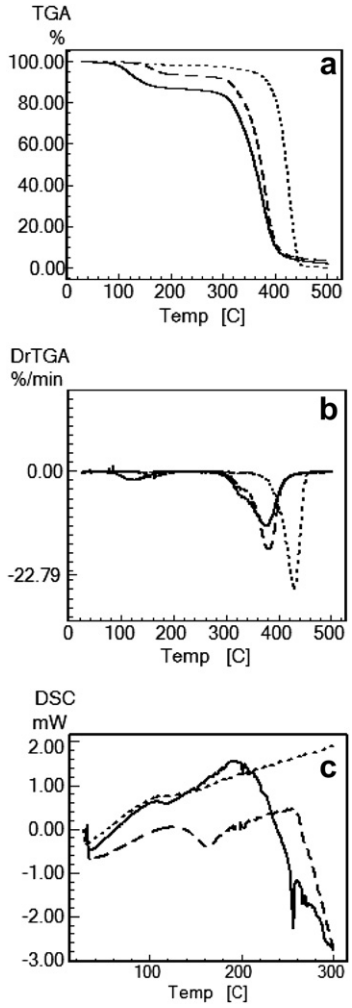


**Fig. 7.** TGA (a), DTG (b) and DSC (c) curves of terpolymer-1 (—), terpolymer-2 (---) and terpolymer-3 (· · · ·).

### 3.6. Dynamic mechanical properties

DMA plots of storage modulus (SM), loss modulus (LM), and tan $\delta$ *vs*. temperature (T) for the terpolymer-1 are shown in Fig. 8(a). SM – T plot shows sharper decrease from 101 to 200 °C with a decreasing SM from 1.2 × 10$^6$ to 1.9 × 10$^4$ MPa. This diminish corresponds to an α-transition with a value of 161 °C. According to the LM – T curve, α-transition is observed at 146, and the tan $\delta$ – T curve α-transition is observed at 151 °C. Certain DMA parameters and first derivatives demonstrated α- or other (sub-$T_g$) transitions and for which the results are summarized in Table 4.

DMA plots of the terpolymer-2 are shown in Fig. 8(b). According to SM–T behavior, a sharp decrease is observed from 117 °C with a value of 1.1 × 10$^6$ MPa–222 °C with a value of 7.5 × 10$^4$ MPa. This decrease corresponds to an α-transition (at 173 °C) and observed from the LM – T and tan $\delta$ – T plots with a value of 173 and 177 °C, respectively. Secondary transitions are also observed and summarized in Table 4.

DMA plots of SM, LM and tan $\delta$ *vs*. T for the terpolymer-3 are shown in Fig. 8(c). Examination of the SM – T behavior of this terpolymer shows multistep decreasing from 1.2 × 10$^6$ to 4.6 × 10$^4$ MPa that starts in the region of 66–185 °C. This broadened peak corresponds to a value of 127 °C and displays a glass transition. According to LM and tan $\delta$, one transition is observed at 129 and 141 °C, respectively, as a broad peak. These transitions may result from

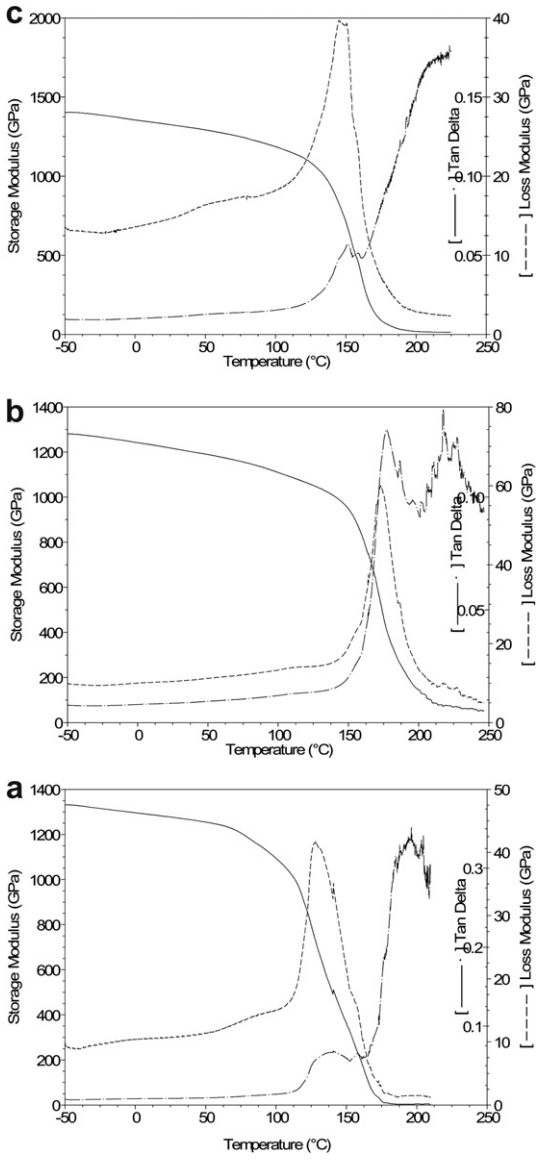


**Fig. 8.** SM, LM, and tan $\delta$ *vs.* temperature plots of terpolymer-1 (a), terpolymer-2 (b) and terpolymer-3 (c).

the α-transition and pseudo-melting behavior of the hydrogen bonded structure. These broadening or multiple peaks indicate that terpolymer has a random structure. Thermal transitions in other viscoelastic parameters are summarized in Table 4. It can be

**Table 4**
DMA parameters of terpolymers.

| DMA parameters | Terpolymer-1 | Terpolymer-2 | Terpolymer-3 |
|---|---|---|---|
| | $T_\alpha$-relaxation (°C) | $T_\alpha$-relaxation (°C) | $T_\alpha$-relaxation (°C) |
| SM | 161 | 173 | 127 |
| DSM | 153, 161 | 163, 173 | 120, 126, 134 |
| LM | 145, 151 | 173 | 129, 133, 141 |
| DLM | 153, 160 | 179, 189 | 138, 144, 150 |
| DFM | 153, 161 | 161, 172 | 119, 126, 133 |
| tan $\delta$ | 151, 158 | 177 (b) | 146 (b) |
| DV | 145, 151 | 173 | 128 |
| DDV | 153, 156 | 179, 189 | 138, 144, 150 |

SM: storage modulus, DSM: deriv. storage modulus, LM: loss modulus, DLM: deriv. loss modulus, DFM: deriv. fluxural modulus, DV: dynamic viscosity, DDV: deriv. dynamic viscosity, b: broad.

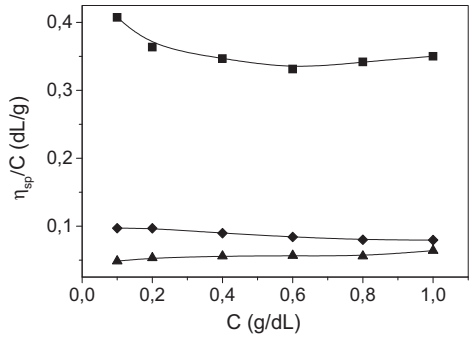


**Fig. 9.** The plots of $\eta_{sp}$/C (reduced viscosity) *vs.* C (concentration) of terpolymer-1 (—▲—), terpolymer-2 (—◆—) and terpolymer-3 (—■—).

concluded that all f(x)-x functions and 1st and 2nd derivatives demonstrate nearly the same values for transitions; glass transitions and pseudo-melting behavior of hydrogen bonding units appearing around at almost the same regions.

All terpolymers show typical viscoelastic behavior of an amorphous polymer. An observed decrease in SM can be interpreted as a softening of the material. No plateau regions and no relaxation processes were observed above $T_g$ in SM–T plot. But in the LM or tan $\delta$ curves, several peaks/transitions were observed at nearly the same temperatures. Higher transition temperature for the terpolymer-2 may signify that the polymer possesses stronger or more efficient dipole–dipole interactions and physically cross-linking of the hydrogen bonded functional groups [2]. In the tan $\delta$ – T plot pseudo-melting peaks of the hydrogen bonded groups can be observed.

### 3.7. Solution properties

According to Fig. 9, terpolymers-2 and 3 exhibit typical polyelectrolyte behavior implying that reduced viscosity decreased with an increase in polyelectrolyte concentration. Especially, terpolymer-3 shows strong polyelectrolyte effect due to the respectively higher amount of VPA units. Reduced viscosities of the terpolymers increase with the increasing VPA content from terpolymer-1 to terpolymer-3. This result is supported by the good agreement with the molecular weights. Molecular weights increase from terpolymer-1 to terpolymer-3. Another approach may again be argued with the increasing VPA content, most probably increasing the intra- and intermolecular interactions between functional groups.

Acid numbers of terpolymers were determined by titration and calculated as 729.3, 650.8 and 235.6 mg KOH/g for the terpolymers 1, 2 and 3, respectively. Hydrolysis of CA in aqueous media increases the acid number of terpolymers.

## 4. Conclusions

Novel functional terpolymers containing VPA have been prepared via complex-radical terpolymerization of $A_1$(CA)-D(S)-$A_2$(VPA) acceptor-donor-acceptor monomer system. Complex formation in CA-S system was investigated and $K_c$ was determined by $^1$H NMR method. Complexed monomer reactivity ratios were determined by $^1$H NMR analysis. Monomer unit compositions of CA, S and VPA in terpolymers were calculated by FTIR. Structure-property relationships of terpolymers and characterization of terpolymers and functional groups were identified by spectroscopic methods. Molecular weights increases with the VPA content. Terpolymers show polydisperse character with values between

2.32 and 2.69. Thermal stability increased with increasing VPA content up to ~500 °C especially for terpolymer-3. Observed pseudo-melting peaks in DSC and in DMA curves can be explained by strong hydrogen bonding effect. Viscosity measurements indicated that VPA containing terpolymers exhibit polyelectrolyte behavior in general, especially for the higher content of the VPA containing terpolymer-3 resulting from the acidic groups.

Reactive and functional poly(CA-*co*-S-*co*-VPA)s which contain anhydride and phosphonic acid units can be used for the future modification and for the new polymer–metal complex systems and potential application in proton exchange materials.

## Acknowledgements

This work was supported by Scientific Research Fund of Hacettepe University (05D11601003) and The Scientific and Technological Research Council of Turkey (TBAG-106T141) which is highly appreciated.

## References

[1] Tan J, Gemeinhard RA, Ma M, Saltzman WM. Biomaterials 2005;26:3663–71.
[2] Wu Q, Weiss RA. J Polym Sci Polym Phys 2004;42:3628–41.
[3] Cho CG, Kim SH, Park YC, Kim H, Park JW. J Membr Sci 2008;308:96–106.
[4] Erdemi H, Bozkurt A. Eur Polym J 2004;40:1925–9.
[5] Kaltbeitzel A, Schauff S, Steininger H, Bingöl B, Brunklaus G, Meyer WH, et al. Solid State Ionics 2007;178:469–74.
[6] Yazawa T, Shojo T, Mineshige A, Yusa S, Kobune M, Kuraoka K. Solid State Ionics 2008;178:1958–62.
[7] Canadell J, Hunt BJ, Cook AG, Mantecon A, Cadiz V. Polym Degrad Stabil 2007;92(8):1482–90.
[8] Rzaev ZMO. Prog Polym Sci 2000;25:163–217.
[9] Yang JZ, Otsu T. Macromolecules 1992;25:102–7.
[10] Zeliazkow MS. Eur Polym J 1999;35:1671–8.
[11] Kahraman G, Beşkardeş O, Rzaev ZMO, Pişkin E. Polymer 2004;45:5813–28.
[12] Kırcı Denizli B, Kaplan Can H, Rzaev ZMO, Güner A. J Appl Polym Sci 2006;100:2455–63.
[13] Rzaev ZM. Polymers and copolymers of maleic anhydride. Baku: Elm; 1984; Chem Abstr 1985;102:11410w.
[14] Cowie JMG. Alternating copolymerization. New York: Plenum Press; 1985.
[15] Keramopoulos A, Kiparissides C. J Appl Polym Sci 2003;88:161–76.
[16] Shoonbrood HA, Van der Reijen B, de Kock JBL, Manders BG, Van Herk AM, German AI. Macromol Rapid Commun 1995;16:119–24.
[17] Boback M, Kowollic C. Macromol Chem Phys 1999;200:1764–70.
[18] Dube MA, Penlidis A. Macromol Chem Phys 1995;196:1101–12.
[19] Gao J, Penlidis A. Macromol Chem Phys 2000;201:1176–84.
[20] Brauer GM, Horowitz E. Systematic procedures. In: Kline GM, editor. Analytical chemistry of polymers, part III. Identification procedures and chemical analysis. New York: Interscience Publishers; 1962. p. 82–5.
[21] Hanna M, Ashbaugh J. J Phys Chem 1964;68:811–6.
[22] Kavlak S, Güner A, Rzaev ZMO. Submitted.
[23] Jaacks VV. Macromol Chem 1967;105:289–91.
[24] Rzaev ZMO, Güner A, Kibarer G, Kaplan Can H, Aşıcı A. Eur Polym J 2002;38:1245–54.
[25] Thomas LC. Interpretation of the infrared spectra of organophosphorous compounds. New York: Heyden & Son Ltd; 1974 [Chapters 3–5, 15].